

- [17] Y. Sun, B. Mayers, T. Herricks, Y. Xia, *Nano Lett.* **2003**, *3*, 955.
- [18] a) Y. Sun, B. Mayer, Y. Xia, *Nano Lett.* **2002**, *2*, 481. b) Y. Sun, B. Mayers, Y. Xia, *Adv. Mater.* **2003**, *15*, 641. c) W. Lin, T. H. Warren, R. G. Nuzzo, G. S. Girolami, *J. Am. Chem. Soc.* **1993**, *115*, 11 644. d) G. S. Métraux, Y. C. Cao, R. Jin, C. A. Mirkin, *Nano Lett.* **2003**, *3*, 519. e) L. A. Porter, Jr., H. C. Choi, A. E. Ribbe, J. M. Buriak, *Nano Lett.* **2002**, *2*, 1067.
- [19] C. J. Johnson, E. Dujardin, S. A. Davis, C. J. Murphy, S. Mann, *J. Mater. Chem.* **2002**, *12*, 1765.
- [20] a) Y. Sun, Y. Xia, *Nano Lett.* **2003**, *3*, 1569. b) H. Shi, L. Zhang, W. Cai, *J. Appl. Phys.* **2000**, *87*, 1572.
- [21] a) Y. Xia, N. Venkateswaran, D. Qin, J. Tien, G. M. Whitesides, *Langmuir* **1998**, *14*, 363. b) K. M. Kulinoski, P. Jiang, H. Vaswani, V. L. Colvin, *Adv. Mater.* **2000**, *12*, 833.
- [22] S.-W. Kim, M. Kim, W. Y. Lee, T. Hyeon, *J. Am. Chem. Soc.* **2002**, *124*, 7642.
- [23] M. Schierhorn, L. M. Liz-Marzán, *Nano Lett.* **2002**, *2*, 13.
- [24] S. J. Oldenburg, R. D. Averitt, S. L. Westcott, N. J. Halas, *Chem. Phys. Lett.* **1998**, *288*, 243.
- [25] J. P. Kottmann, O. J. F. Martin, D. R. Smith, S. Schultz, *Phys. Rev. B* **2001**, *64*, 235 402.
- [26] L. R. Hirsch, J. B. Jackson, A. Lee, N. J. Halas, J. L. West, *Anal. Chem.* **2003**, *75*, 2377.
- [27] Y. Xia, P. Yang, Y. Sun, Y. Wu, B. Mayers, B. Gates, Y. Yin, F. Kim, H. Yan, *Adv. Mater.* **2003**, *15*, 353.

Receptor-Mediated Self-Assembly of Multi-Component Magnetic Nanowires**

By Aliasger K. Salem, Johnny Chao, Kam W. Leong, and Peter C. Searson*

The bottom-up approach to the miniaturization of devices requires spatial control over the arrangement and assembly of nanoscale building blocks.^[1–3] As a result of advances in the synthesis of nanoscale building blocks, there is an increasing interest in techniques to induce self-assembly. In addition to directing the spatial location and placement of building blocks, the subsequent ability to manipulate the building blocks is equally important.

Nanowire building blocks are of particular interest since their inherent shape anisotropy offers additional degrees of freedom for manipulation compared to spherical particles.^[4] Furthermore, the introduction of multiple segments along the length of a nanowire can lead to additional versatility asso-

ciated with the ability to introduce multiple chemical functionalities.^[5–7] The ability to form self-assembled monolayers with surface-specific linkages has been exploited for directed self-assembly and sensing.^[8,9]

In this paper we demonstrate the directed orientation of ferromagnetic nanowires tethered to spatially controlled regions of a surface. The ability to selectively functionalize specific segments in multi-segment nanowires is used to direct the binding of the nanowires to specific regions on the surface. By incorporating a rod-shaped ferromagnetic segment with high aspect ratio, the shape anisotropy leads to a magnetic easy axis parallel to the wire axis, and hence allows control of the spatial orientation of the nanowires in an external field.

Two segment Au/Ni nanowires were anchored to the surface using the biotin-avidin linkage. This linkage is one of the strongest known biological interactions with a binding constant of 10^{-15} M⁻¹ and stability over a broad pH range.^[10,11] Patterned regions of the avidin were introduced using a microfluidic patterning technique. This is a method that has found wide utility in a variety of applications from patterning of proteins^[12] and cells^[13] to the physical positioning of nanowires.^[14,15]

Figure 1 shows schematically our approach for synthesis and assembly of patterned magnetic nanowire arrays. First, an evaporated silver film was biotinylated by incubation in a 0.1 mg mL⁻¹ solution of *N*-([6-biotin-amido]hexyl)3'-[2'-pyridylthio]propionamide in trifluoroethanol. Next, avidin was bound to specific regions of the biotinylated silver surface using a poly(dimethylsiloxane) (PDMS) mold with channels ranging from 7 to 10 μ m in width. The mold was placed onto the biotinylated silver surface and 2 mL of a 250 μ g mL⁻¹ solution of NeutraAvidin tetramethyl rhodamine (NATR) (Molecular Probes) was placed at the entrance of the capillaries. A negative pressure was applied at the other end to draw the avidin solution through the channels. After 30 min, the channels were flushed by drawing 3 mL deionized water through the channels under negative pressure. This process was repeated 10 times. The PDMS stamp was then removed and the biotinylated silver surface further rinsed with deionized water. The coupling of avidin to the biotinylated surface in the channels provides a binding point for the biotinylated gold segments of the nanowires.

Two-segment Au/Ni nanowires were fabricated by electrochemical template synthesis. The nanowires were 170 nm in diameter and 9 μ m in length, with 1 μ m long gold segments and 8 μ m long nickel segments, as shown in the backscattered scanning electron microscopy (SEM) image in Figure 2A. In these images, the gold segment was longer than required for anchoring to the surface in order to facilitate imaging of the selective functionalization.

A solution of thiol-terminated biotin was added to a suspension of the Au/Ni nanowires at a concentration of 0.005 M. Then after 24 h, the nanowires were transferred to deionized water by repeated centrifugation and re-suspension. NATR was then added in excess to the nanowire suspension for 5 min, followed by transfer to deionized water. Fig-

[*] Prof. P. C. Searson, J. Chao
Department of Materials Science and Engineering
Johns Hopkins University
Baltimore, MD 21218 (USA)
E-mail: searson@jhu.edu

Dr. A. K. Salem, Prof. K. W. Leong
Department of Biomedical Engineering
Johns Hopkins University
Baltimore, MD 21218 (USA)

[**] This work was supported by DARPA/AFOSR (under grant number F49620-02-1-0307).

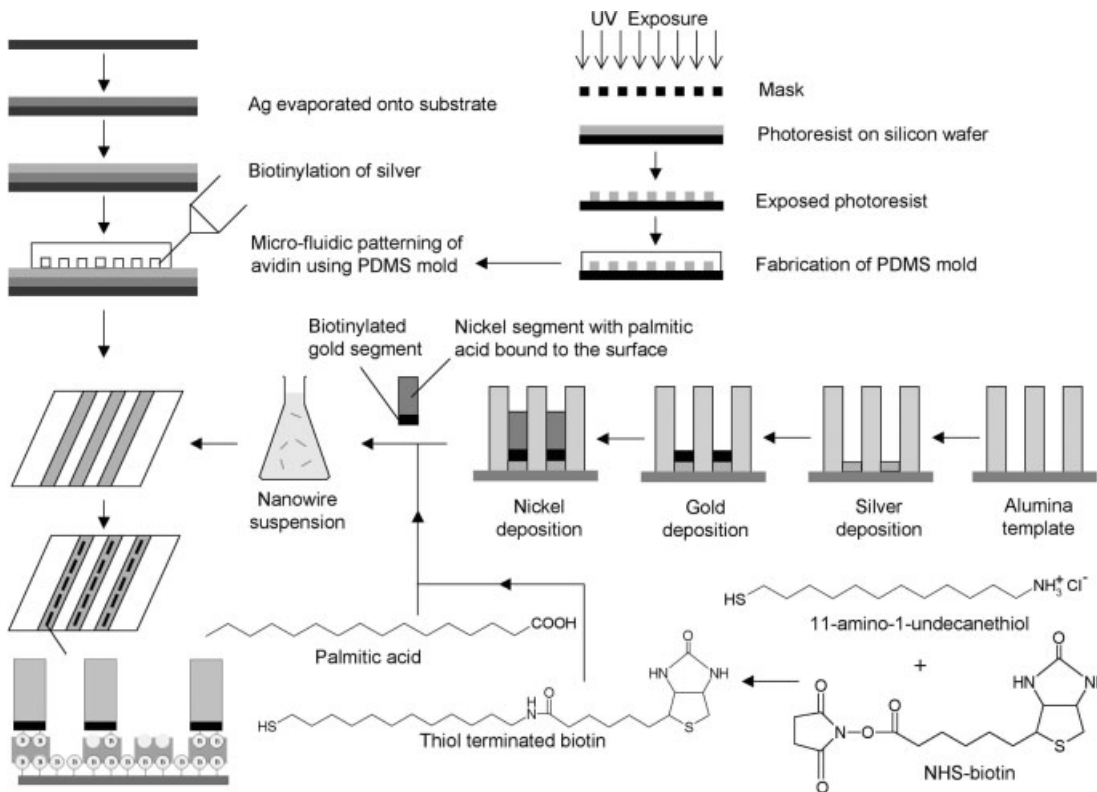


Figure 1. Schematic of magnetic nanowire array preparation.

ures 2B,C show the corresponding light microscope and fluorescence images of the functionalized nanowires. The fluorescence image in Figure 2C shows that the NATR (absorption: 555 nm, emission: 580 nm) was bound to the gold segment along with a significant amount of non-specific binding along the nickel segment. This suggests that there is weak binding of the thiol-terminated biotin to the nickel segments.

In order to eliminate the non-specific binding, palmitic acid was bound to the native oxide on the nickel segments. A mixture of palmitic acid and thiol-terminated biotin was added to the nanowire suspensions at an equimolar concentration of 0.005 M. Carboxylic acid groups are known to bind selectively to metal oxides, including the native oxide on transition metals.^[16,17] Figures 2D,E show corresponding light microscope and fluorescence images after incubating the nanowires in NATR. The fluorescence image clearly shows selective binding of the NATR on the gold segment, illustrating that the palmitic acid binds preferentially on the native oxide of the nickel segments to block the non-specific binding of the thiol-terminated biotin.

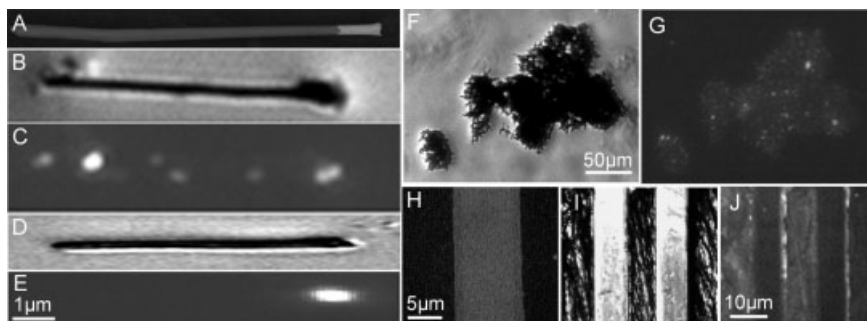


Figure 2. A) Back-scattered SEM image showing a two-segment Au/Ni nanowire with a 1 μm gold segment and an 8 μm nickel segment. B) Light microscope image of a two-segment Au/Ni nanowire functionalized with biotinylated thiol and NATR; C) corresponding fluorescence image showing that NATR is bound non-specifically along the whole length of the nanowire. D) Light microscope image of a two-segment Au/Ni nanowire functionalized with palmitic acid and biotinylated thiol followed by NATR; E) corresponding fluorescence image showing NATR bound specifically to the Au segment. F) Light microscope image of aggregated biotinylated nanowires; G) corresponding fluorescence image showing aggregation mediated by the NATR. H) Fluorescence image showing 10 μm wide patterned tracks of rhodamine labeled NATR. I) Light microscope images show that nanowires are immobilized within the tracks; J) corresponding fluorescence image showing emission from NATR localized to the patterned tracks.

We note that the addition of excess NATR to the nanowire suspension is essential to saturate the biotin sites and hence avoid nanowire–nanowire binding. Aggregation of the biotinylated nanowires was observed when NATR was added to the suspension in small incremental amounts starting with 10 μL of a 10 μg mL⁻¹ solution, as shown in Figure 2F. Fluorescence images show that the aggregation is mediated by the NATR (Fig. 2G). Incremental addition

of avidin increases the fraction of nanowires unsaturated with avidin and hence increases the probability of nanowire–nanowire binding.

Following selective functionalization of the biotinylated gold segments, the nanowires were spin-coated onto the avidin patterned substrates from suspension at 2500 rpm for 15 s. After 5 min of standing, the substrate was washed thoroughly, and the nanowires were shown to selectively bind only to regions patterned with the fluorescently labeled avidin (Fig. 2I,J).

In order to demonstrate that the nanowires were tethered to the avidin tracks, the samples were immersed in water and a small magnetic field was applied either parallel or perpendicular to the tracks using a NdFeB magnet, as illustrated in Figure 3. The aspect ratio of the nickel segments is about 50, and hence the magnetic easy axis is parallel to the wire axis. When the magnetic field was applied parallel to the tracks, the nanowires rotated so that the nickel segments were

aligned parallel to the field, as shown in Figure 3A. Similarly, when the field was applied perpendicular to the tracks, the nanowires rotated to be parallel to the field and perpendicular to the tracks. Fluorescence images confirmed that the nanowires were still anchored within the rhodamine-labeled avidin patterned regions (Fig. 3C).

In summary, we have demonstrated molecular self-assembly and external manipulation of multifunctional magnetic nanowires in spatially localized regions using a microfluidic-based approach combined with selective surface functionalization. This approach has potential for applications ranging from self-assembly of intricate macrostructures to biosensors that utilize protein-based nanoscale switches.

Experimental

The thiol-terminated biotin was synthesized by reacting 10 mg 11-amino-1-undecanethiol (Dojindo) with 14.2 mg *N*-hydroxy-succinimide-biotin (Sigma) in 5 mL of a 50:50 mixture of dimethylformamide and dimethylsulfoxide overnight under an argon blanket at room temperature.

The mold was fabricated by curing a prepolymer (Sylgard Silicone Elastomer-184, Dow Corning) on a patterned master, which was prepared by spin-coating 250 μL photoresist (SU8) onto a silicon wafer for 55 s at 2500 rpm, solvent-baked at 100 $^{\circ}\text{C}$ for 100 s, and then exposed to UV light (100 mJ cm^{-2}) from a mercury vapor lamp. The exposed resist was developed in a 4:1 mixture of de-ionized water and developer (AZ-400 K, Clariant Corp., NJ). Following rinses with de-ionized water and drying with nitrogen, the patterned master was then hard-baked for 25 min at 125 $^{\circ}\text{C}$. The elastomeric mold with the negative pattern of the master imprinted on it was peeled off and washed several times with ethanol, hexane, and deionized water.

Nanowires were fabricated by electrodeposition into an Al_2O_3 template (Anodisc, Whatman) with a nominal pore diameter of 100 nm. An evaporated silver film on one side of the template served as the working electrode in a three-electrode configuration. A thin layer of silver was first electrodeposited from 50 mM $\text{KAg}(\text{CN})_2$ and 0.25 M Na_2CO_3 buffered to pH 13 at a potential of -1.0 V (Ag/AgCl) in order to ensure easy release of the nanowires from the template. The Au segments were deposited from a commercial gold plating solution (Technic) at a potential of -1.0 V (Ag/AgCl) and the Ni segments were deposited from a solution of 20 g L^{-1} $\text{NiCl}_2 \cdot 6\text{H}_2\text{O}$, 515 g L^{-1} $\text{Ni}(\text{H}_2\text{NSO}_3)_2 \cdot 4\text{H}_2\text{O}$, 20 g L^{-1} H_3BO_3 buffered to pH 3.4 at a potential of -1.0 V (Ag/AgCl). The silver layers were dissolved in 70 vol.-% nitric acid and the alumina template was then dissolved in 2 M KOH. Note that the gold segments were deposited before the nickel segments in order to ensure that the nickel segments were not etched by the nitric acid during removal of the silver. The nanowires were washed repeatedly using 2 M KOH, de-ionized water, and ethanol.

In control experiments biotinylated nanowires did not bind to avidin tracks pre-saturated with d-biotin. Similarly, nanowires with biotin binding sites pre-saturated with avidin did not bind to the patterned avidin tracks. These experiments confirm that the nanowires were specifically bound to the surface through the biotin–avidin linkage.

Received: July 15, 2003
Final version: October 12, 2003

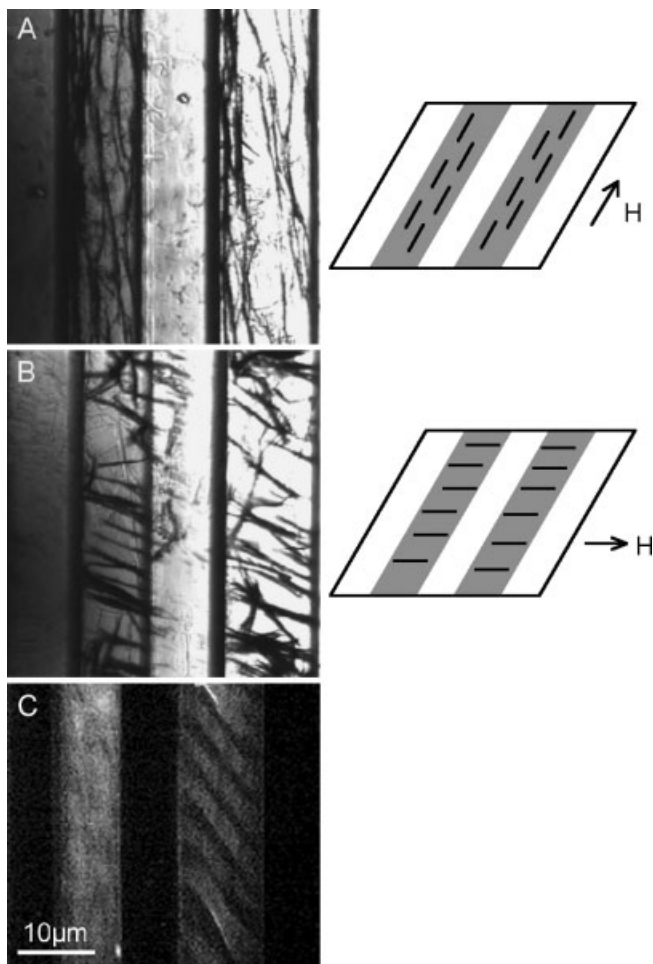


Figure 3. A) Light microscope image of two-segment Au/Ni biotinylated nanowires immobilized on patterned avidin tracks in an aqueous environment with an applied magnetic field parallel to the tracks; B) corresponding light microscope image with the applied magnetic field perpendicular to the tracks. C) Fluorescence image confirms that the nanowires remain within the patterned tracks of fluorescently labeled avidin.

- [1] A. Amma, B. Razavi, S. K. St Angelo, T. S. Mayer, T. E. Mallouk, *Adv. Funct. Mater.* **2003**, *13*, 365.
- [2] S. A. Sapp, D. T. Mitchell, C. R. Martin, *Chem. Mater.* **1999**, *11*, 1183.
- [3] S. Mann, W. Shenton, M. Li, S. Connolly, D. Fitzmaurice, *Adv. Mater.* **2000**, *12*, 147.

- [4] M. Chen, L. Sun, J. E. Bonevich, D. H. Reich, C. L. Chien, P. C. Searson, *Appl. Phys. Lett.* **2003**, *82*, 3310.
- [5] S. R. Nicewarner-Pena, R. G. Freeman, B. D. Reiss, L. He, D. J. Pena, I. D. Walton, R. Cromer, C. D. Keating, M. J. Natan, *Science* **2001**, *294*, 137.
- [6] B. R. Martin, D. J. Dermody, B. D. Reiss, M. M. Fang, L. A. Lyon, M. J. Natan, T. E. Mallouk, *Adv. Mater.* **1999**, *11*, 1021.
- [7] A. K. Salem, P. C. Searson, K. W. Leong, *Nat. Mater.* **2003**, *2*, 668.
- [8] J. K. N. Mbindyo, B. D. Reiss, B. R. Martin, C. D. Keating, M. J. Natan, T. E. Mallouk, *Adv. Mater.* **2001**, *13*, 249.
- [9] C. A. Mirkin, R. L. Letsinger, R. C. Mucic, J. J. Storhoff, *Nature* **1996**, *382*, 607.
- [10] A. K. Salem, S. M. Cannizzaro, M. C. Davies, S. J. B. Tendler, C. J. Roberts, P. M. Williams, K. M. Shakesheff, *Biomacromolecules* **2001**, *2*, 575.
- [11] E. P. Diamandis, T. K. Christopoulos, *Clin. Chem. (NY)* **1991**, *37*, 625.
- [12] E. Delamarche, A. Bernard, H. Schmid, B. Michel, H. Biebuyck, *Science* **1997**, *276*, 779.
- [13] N. Patel, R. Padera, G. H. W. Sanders, S. M. Cannizzaro, M. C. Davies, R. Langer, C. J. Roberts, S. J. B. Tendler, P. M. Williams, K. M. Shakesheff, *FASEB J.* **1998**, *12*, 1447.
- [14] B. Messer, J. H. Song, P. D. Yang, *J. Am. Chem. Soc.* **2000**, *122*, 10232.
- [15] Y. Huang, X. F. Duan, Q. Q. Wei, C. M. Lieber, *Science* **2001**, *291*, 630.
- [16] M. Tanase, L. A. Bauer, A. Hultgren, D. M. Silevitch, L. Sun, D. H. Reich, P. C. Searson, G. J. Meyer, *Nano Lett.* **2001**, *1*, 155.
- [17] D. L. Allara, R. G. Nuzzo, *Langmuir* **1985**, *1*, 45.

Highly Efficient Biocatalysts via Covalent Immobilization of *Candida rugosa* Lipase on Ethylene Glycol-Modified Gold–Silica Nanocomposites

By Ulf Drechsler, Nicholas O. Fischer, Benjamin L. Frankamp, and Vincent M. Rotello*

The immobilization of biomolecules onto insoluble supports is an important tool for the fabrication of a diverse range of functional materials or devices.^[1] These bioconjugates have found numerous applications in the areas of biocatalysis,^[2] sensing,^[3] and biomedicine.^[4] Many of these applications require high surface to volume ratios, an inherent feature of nanoscale materials, making nanostructured systems attractive candidates as scaffolds for enzymes, proteins, or nucleic acids.^[5] Many potential materials, however, lack biocompatible surfaces, leading to rapid denaturation and thus sharply decreased activity of surface-bound biomolecules.^[6] While this issue can be overcome through appropriate surface modi-

fication, this can prove difficult for many materials, resulting in substantial losses in enzymatic activity.^[7] The facile deposition of thiol-terminated molecules onto gold surfaces, on the other hand, presents an attractive approach to introduce desired surface functions.^[8]

Recently, we reported the fabrication of silica–noble metal composites obtained through versatile polymer-mediated nanoparticle self-assembly. This modular ‘bottom-up’ approach provides control over the aggregate morphology through stoichiometry, polymer and nanoparticle composition, and the order of addition of the individual components.^[9] Subsequent calcination leads to complete removal of all organic constituents, leaving behind dispersed metal clusters on the surface that are highly efficient catalysts for hydrogenation.^[10] In addition to serving as catalysts in their own right, an alternative application of these dispersed metal clusters is as platforms for further surface functionalization. In this paper we report the modification of these nanoparticle aggregates and their application as supports for the creation of highly active supported biocatalysts based on the *Candida rugosa* lipase (CRL).

Among the many enzymes used in biocatalytic processes, lipases have gained particular interest as catalysts in organic synthesis. These hydrolytic enzymes are relatively insensitive towards non-aqueous solvents, can tolerate fairly broad pH and temperature ranges, and most importantly, exhibit high chemoselectivities.^[11] Lipases have found applications ranging from kinetic asymmetric resolutions^[12] to polymerizations.^[13]

The gold–silica nanocomposites used in this study were fabricated from 15 nm carboxy-functionalized silica particles, a random copolymer of styrene and aminomethylstyrene, and 2 nm carboxy-functionalized gold nanoparticles, as previously described.^[9] Calcination at 500 °C gave the inert nanocomposite carrier material (Fig. 1).^[14] In a preliminary study,

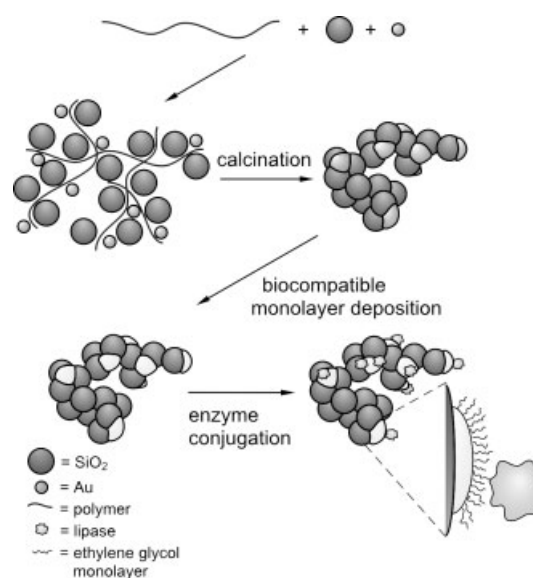


Figure 1. Schematic illustration of lipase biocatalyst fabrication based on “bricks and mortar” nanoparticle assembly.

* Prof. V. M. Rotello, Dr. U. Drechsler, N. O. Fischer, B. L. Frankamp
Department of Chemistry, University of Massachusetts
Amherst, MA 01003 (USA)
E-mail: rotello@chem.umass.edu

[**] This research was supported by the NIH (GM62998) and the NSF (DMR-0213695, MRSEC).